scientific reports

Check for updates

OPEN

Green synthesis and characterization of TiO_2 nanoparticles from latex of *Calatropis procera* against dusky cotton bug

Maham Fatima[3], Tehmina Anjum[1], Mujahid Manzoor[2], Muzammil Aftab[4]✉, Zill-e-Huma Aftab[1]✉, Waheed Akram[1], Najat A. Bokhari[5], Humaira Rizwana[5], Ghulam Nabi[1] & Guihua Li[6]

The dusky cotton bug is a small insect that poses a significant threat to cotton crops. Due to increasing reports on the development of resistance in this insect against insecticides, efforts to control this pest must involve other environment-friendly strategies. The use of nanoparticles (NPs) has generated an alternative pest control. The objective of this study was to evaluate the insecticidal effect of green synthesized titanium dioxide nanoparticles (TiO_2) NPs using latex of *Calatropis procera* against dusky cotton bug 2nd and 4th instar nymph and adult stage. The optical properties of the synthesized nanoparticles were confirmed through UV-Vis spectroscopy whereas, surface morphology was checked through Scanning Electron Microscopy. A detailed XRD analysis of the synthesized particles confirmed that the particles belong to the anatase phase, of the tetragonal crystal system. When checked for their insecticidal potential against dusky cotton bugs (2nd and 4th instar nymph and adult stage) through the leaf dip method, the nanoparticles-controlled insect population was up to 95% with highest in 2nd instar nymphs and lowest in adults. However, the insecticidal activity was found directly proportional to the concentration of nanoparticles used.

Keywords Nanotechnology, Cotton, Green synthesis, *Oxycarenus* spp.

The dusky cotton bug (*Oxycarenus* spp.), a common pest of cotton, okra, and other plants of the Malvaceae family belongs to the family Lygaeidae. Species of *Oxycarenus* have been reported in Pakistan, India, Iraq, Myanmar, Malaysia, Cambodia, Vietnam, and Laos. This species, generally known as the cotton seed bug, lodge a similar niche in other cotton-growing areas of the world[1]. Smith and Brambila[2] reported high population densities of dusky cotton bugs in Florida. Reports are also available confirming its presence in Turkey, Caicos, Bahamas, Cayman Islands[3–5].

The dusky cotton bug is emerging as an important pest of cotton in various cotton-growing countries including Pakistan. The pest gets crushed in the ginning process and stains cotton lint with a pink color resulting in a low value of the product[6]. The introduction of Bt cotton has reduced the use of pesticides including organophosphate and pyrethroids, because of which the dusky cotton bug has emerged as a major pest of cotton in the last few years. Both mature as well as immature life stages of this pest damage the crop and reduce the yield, seed weight, and oil contents through sucking cell sap[7]. Sewify and Semeada[8] reported a 32% reduction in cotton seed weight with 6% less oil production due to this bug. The viability of the seeds is also known to be reduced by this bug as it damages seed embryos[9].

Cotton growers are heavily relying on insecticides against dusky cotton bug[10]. However, species of dusky cotton bug have shown high potential to develop resistance against several pesticides. Ullah, et al.[11] reported

[1]Department of Plant Pathology, Faculty of Agricultural Sciences, University of the Punjab, Lahore, Pakistan. [2]Department of Entomology, Faculty of Agricultural Sciences, University of the Punjab, Lahore, Pakistan. [3]Institute of Zoology, University of the Punjab, Lahore, Pakistan. [4]Department of Physics, Government Shah Hussain College, Chuhang, Lahore, Pakistan. [5]Department of Botany and Microbiology, College of Science, King Saud University, Riyadh 11495, Saudi Arabia. [6]Vegetable Research Institute, Guangdong Academy of Agricultural Sciences, Guangzhou 510640, China. ✉email: m.muzamilaftab@gmail.com; huma.dpp@pu.edu.pk

a 2–30-fold range of resistance in different field populations of *Oxycarenus hyalinipennis* to conventional insecticides including bifenthrin, lambda-cyhalothrin, triazophos, deltamethrin, profenofos, whereas, this range was between 5 and 46 for novel chemistry compounds including emamectin benzoate, nitenpyram, spinosad, imidacloprid, chlorfenapyr. Similarly, Ijaz and Shad[12] predicted the risk of resistance development to spirotetramat. A field-collected population developed a 1230-fold spirotetramat resistance after selection of 19 generations with spirotetramat when compared with the Lab population. Results showed that 11 generations would be required for a 10-fold increase in spirotetramat resistance with insect mortality of 50%. Besides this issue of resistance development, and increasing awareness regarding the harmful effects of pesticides, people all around the world are shifting from chemical-based agriculture to green agriculture. The green extract has been a great choice for researchers due to their marvelous insecticidal activities. Elrehawy and ElDoksch[13] reported a remarkable insecticidal potential of *C. Procera* Latex and leaf extract. Kumar, et al.[14] also explored the insecticidal activity of different extracts of *C. Procera* showing a significant lethality.

Nanotechnology has shown promising potential to support sustainable agriculture. Nano-pesticides are transforming crop production, enabling the development of a new generation of pesticides aimed at reducing negative environmental impacts while maintaining crop yields. Increased efficacy due to their reduced size, stability of formulations and enhanced bioactivity has made nano-pesticides popular in agriculture. Various metal and metal oxide nanomaterials have been checked against various crop pathogens and insects[15–18]. The green synthesis of nanoparticles has made them even more environmentally friendly than conventional nanopesticides manufactured through chemical procedures, due to their minimal residual and hazardous effects. Javaid, et al.[19] used green synthesized silver nanoparticles from *A. indica* to control *O. hyalinipennis*. Shyam-Sundar, et al.[20] developed eco-friendly approach for the biosynthesis of TiO_2 Nanoparticle using *Desmostachya bipinnata* extract for larvicidal and pupicidal efficacy against *Aedes aegypti* and *Spodoptera litura*.

Titanium dioxide nanoparticles are receiving significant attention for their reported antibacterial, antifungal, UV-filtering characteristics, and extraordinary catalytic as well as photochemical activities[21–23]. Many researchers have also reported their positive effects on plant germination and growth[24–26]. Rajam, et al.[27] reported an increase of 20% in plant productivity when treated with titanium dioxide nanoparticles. Few reports are available on the effect of TiO_2 nanoparticles on plant pests that includes studies by Gutiérrez-Ramírez, et al.[28] against *Bactericera cockerelli* and reports of Hilal, et al.[29] and Sabbour[30] against *Tribolium castaneum* and *Sitophilus oryzae* respectively. This research was aimed to explore the synthesis of TiO_2NPs by *Calatropis procera* latex and evaluate its efficiency in controlling. In the light of above stated facts, the present study was planned to explore the insecticidal efficacy of TiO_2 nanoparticles synthesized from *C. procera* extract against Dusky Cotton Bug, as well as the effects of TiO_2 NPs on mortality.

Results

Characterization of NPs using UV-Vis spectroscopy and SEM analysis

The optical properties of the synthesized TiO_2 nanoparticles were studied through UV-Vis spectroscopy. Figure 1 shows the absorbance of the solution in the nano range at room temperature. The sample showed good absorbance at the UV region with a peak at 353 nm. The band gap of TiO_2 has been calculated (3.2 eV) which is found to be in close approximation with the one reported in the literature[31].

The surface morphology of the green synthesized TiO_2 particles was characterized by SEM analysis as shown in Fig. 2. Figure 2 depicts the random shape of particles but as the image is magnified (Fig. 2) one can see the spherical shape of the particles with good dispersion. This type of behavior has already been reported in the literature[32,33]. In addition, less agglomeration of nanoparticles has also appeared, which may be due to the aggregation of TiO_2 particles.

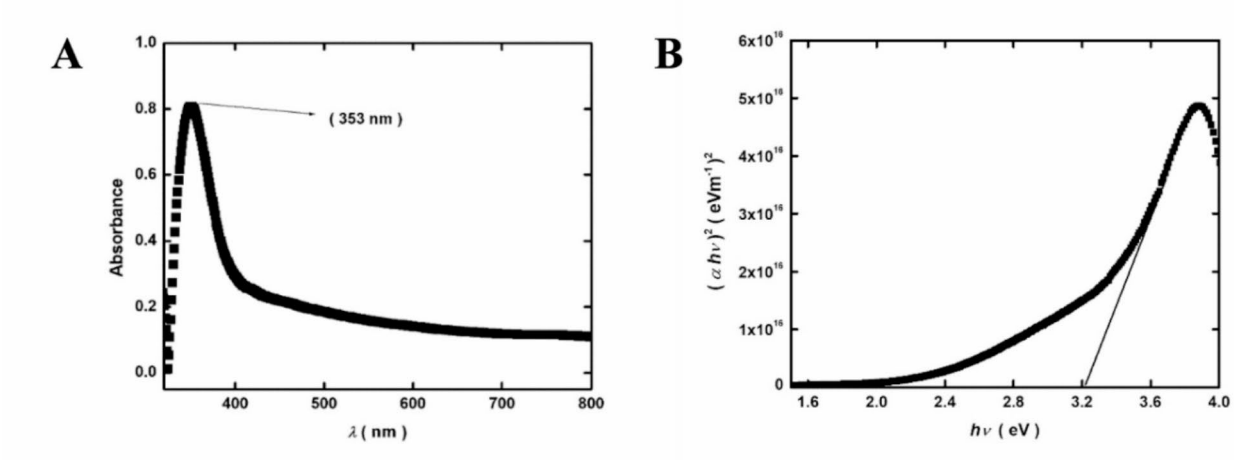

Fig. 1. UV-vis spectrophotometric plot and Band gap of TiO_2 nanoparticles. (**A**) UV-vis spectrophotometric plot showing the absorbance spectra of green synthesized TiO_2 NPs. (**B**) Band gap of TiO_2 nanoparticles from UV-Vis absorption spectroscopy by using Tauc Plot.

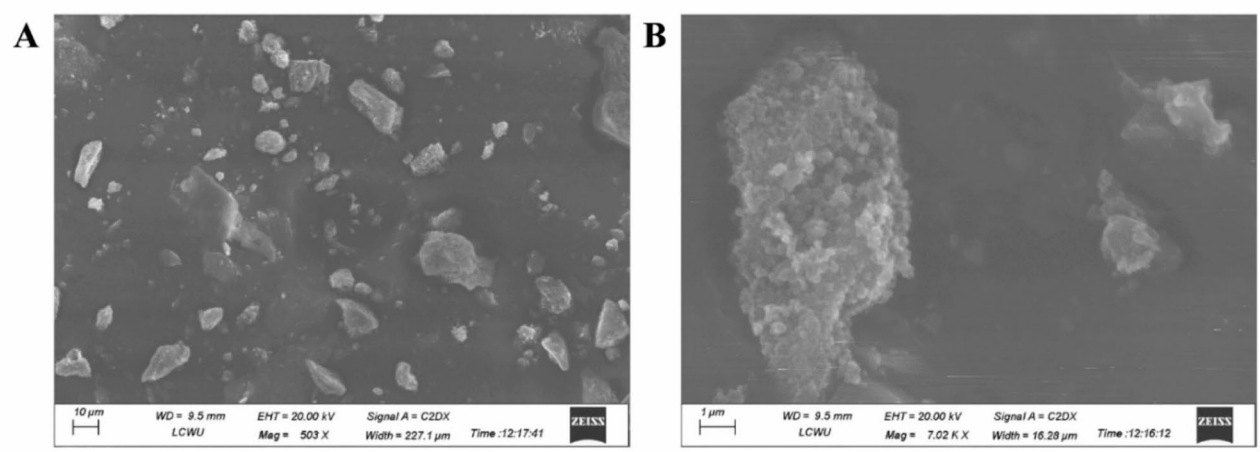

Fig. 2. Scanning electron micrograph of green synthesized TiO_2 NPs. (**a**) 500 X; (**b**) 7 kX.

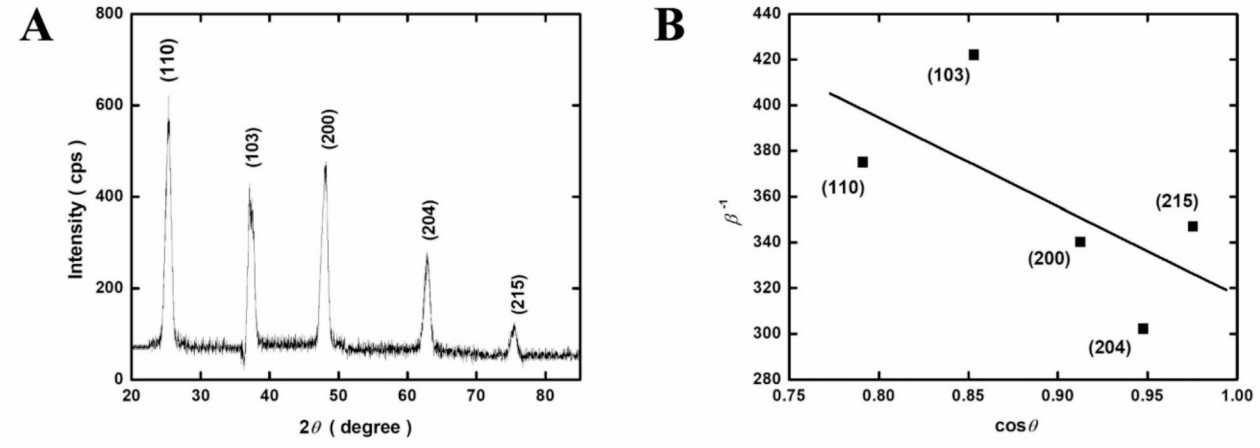

Fig. 3. XRD pattern (**a**) and Scherrer plot (**b**) for TiO_2 nanoparticles.

XRD pattern

Before starting the XRD characterization of TiO_2 nanoparticles, correction for background or instrumental broadening was done in a standard way by recording the diffraction pattern of the instrumental standard Silicon (Si) sample which contributes no sample related line broadening. The instrumental setup was identical to that used for recording the diffraction pattern of TiO_2 nanoparticles. As TiO_2 literature reports, the most prominent peaks have been found in 2θ range of 20° to 80° that is why this range was opted. The most optimum conditions for the X-ray diffractometer used in our case are providing the generator voltage 40 kV and tube current 40 mA keeping the scan step size was 0.02° and time as 4°/min. Figure 3 shows the XRD pattern of TiO_2 nanoparticles. All the peaks have been found in good agreement with the standard reference pattern (JCPDS 89-4921)[34–36]. These nanoparticles belong to the anatase phase, of the tetragonal crystal system. One can see the characteristic peaks of TiO_2 nanoparticles at the 2θ peak positions of 25.42° (110), 37.21° (103), 37.8° (004), 48.25° (200), 62.87° (204), and 75.41° (215)[34].

Evaluation of structural parameters

In literature, several models have been reported to evaluate the structural parameters, i.e. crystallite size and lattice strain. We used the Scherrer equation plot[37], Williamson–Hall analysis (W-H)[38,39], Size–Strain plot (S-S)[40,41], Halder–Wagner equation (H-W)[42,43], and Wagner–Aqua plot (W-A)[44,45] for the evaluation, and compare the values obtained by these methods.

Scherrer equation plot

The Scherrer method is one of the most used methods to calculate the crystallite size of a given specimen[46]. The general form of Scherrer equation is given as:

$$D = \frac{k\lambda}{\beta\, cos\theta}$$

This method provides the crystallite size values for the most prominent peak. But in Scherre plot approach[47,48], all the obtained peaks in the XRD pattern are taken into account. This is done by plotting β^{-1} (FWHM) as a function of *cosθ* for all the diffraction peaks considering the rearranged form Scherrer equation given as:

$$\beta^{-1} = \frac{D}{k\lambda}\ (cos\theta\ )$$

The slope of the fitted straight line gives the average value of the crystallite size of the specimen. Referring to Fig. 3 Scherrer Plot of TiO_2 nanoparticles has been given. The straight line is fitted through the data points by the least-squares fitting method. The obtained value of *D* has been listed in Table 1.

Williamson-Hall analysis

W–H method has been widely used to determine the structural parameters considering both the contributors of peak broadening given as[49,50]:

$$\beta\ = \beta_{\ D} + \beta_{\ \epsilon}\ = \frac{k\lambda}{\mathrm{D}cos\theta} + 4\epsilon\ \tan\theta$$

where $\beta_{\ D}$ is the contribution from crystallite size following the Scherrer equation given above. On the other hand $\beta_{\ \epsilon}$ is the contributing from lattice strain following the Wilson formula $\beta_{\ \epsilon}\ = 4\epsilon\ \tan\theta$. The above expression is the general form of W–H analysis. We have carried out W–H analysis for TiO_2 nanoparticles assuming all the models i.e. UDM (uniform deformation model), UDSM (uniform deformation stress model), and UDEDM (uniform deformation energy density model).

Uniform deformation model (UDM)

In this model, the lattice strain ε throughout the crystal structure is assumed to be uniform therefore the general equation of W– H analysis can be rewritten as:

$$\beta\ \cos\theta\ = \frac{k\lambda}{\mathrm{D}} + 4\epsilon\ \sin\theta$$

Plotting $\beta\ \cos\theta$ as a function of $4\sin\theta$ followed by a statistical linear fit to the data points by the least-squares-fitting method. The intercept of the plot on the y-axis will provide the value of crystallite size whereas the slope provides lattice strain ε (Fig. 4). The obtained values of *D* and ε have been given in Table 1.

Uniform deformation stress model (UDSM)

UDSM considers the anisotropic nature of the crystal presuming uniform lattice stress σ in all crystallographic directions following Hook's law i.e. $\sigma \propto \varepsilon$ or $\sigma = \varepsilon E$, where *E* (also written as E_{hkl}) is the modulus of elasticity[51]. Under these conditions, the general equation of W–H model becomes

$$\beta\ cos\theta\ = \frac{k\lambda}{D} + \sigma\ \left(\frac{4sin\theta}{E_{hkl}}\right)$$

Substituting the values of *E* for all the planes a plot is drawn between $\beta\ cos\theta$ (along y-axis) and $\frac{4sin\theta}{E_{hkl}}$ (along x-axis) in Fig. 4. The slope of the graph provided the value of strain ($\varepsilon = \frac{\sigma}{\mathrm{E}}$ whereas y-intercept gave the crystallite size as given in Table 1.

Uniform deformation energy density model (UDEDM)

UDEDM being the third variant of W-H analysis presumes the energy density *u* given as ($u = \frac{E_{hkl}}{2}\epsilon^{\ 2}$) so the general equation of W-H analysis takes the form (Rosenberg, 2000):

$$\beta\ cos\theta\ = \frac{k\lambda}{D} + 4sin\theta\left(\frac{2u}{E_{hkl}}\right)^{\frac{1}{2}}$$

Scherrer plot	Willamson-Hall analysis						Size-strain plot		Halder-Wagner plot		Wagner Aqua plot	
	UDM		UDSM		UDEDM							
D (nm)	*D*(nm)	$\varepsilon\ (10^{-4})$	*D*(nm)	$\varepsilon\ (10^{-4})$	*D*(nm)	$\varepsilon\ (10^{-4})$	*D*(nm)	$\varepsilon\ (10^{-4})$	*D*(nm)	$\varepsilon\ (10^{-4})$	*D*(nm)	$\varepsilon\ (10^{-4})$
56.293	39.8943	6.4537	44.6964	8.7273	40.5648	2.1527	69.2901	2.1269	54.4422	5.6509	46.4066	9.9309

Table 1. Structural parameters obtained using Scherrer, W-H analysis, SS plot, H. Wagner and W. Aqua plot methods.

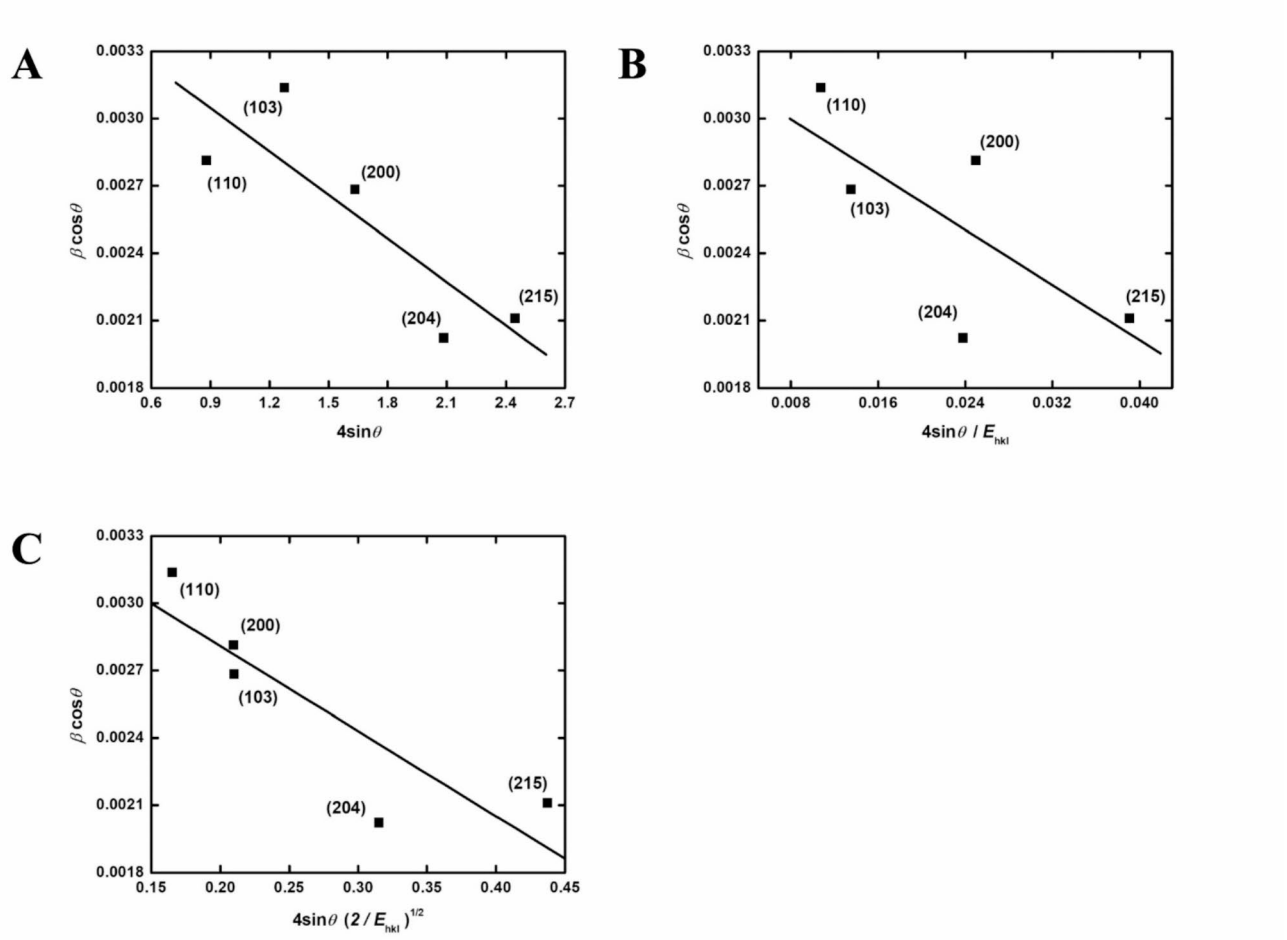

Fig. 4. UDM (**a**), UDSM (**b**), and UDEDM (**c**) plots for TiO_2 nanoparticles.

Figure 4 shows the plot of $\beta\, cos\theta$ vis a vis $4sin\theta \left(\frac{2}{E_{hkl}}\right)^{\frac{1}{2}}$ for TiO_2 nanoparticles. Crystallite size (D) and strain ($\epsilon = \sqrt{\frac{2u}{E_{hkl}}}$) were calculated from the intercept and the slope of the plot respectively and the obtained values have been tabulated in Table 1 as well.

Size–strain plot (SSP) model

The SSP model is a more reliable and suitable approach for the specimens with isotropic line broadening. This model is embodied in the mathematical expression[41,52]:

$$(d\beta\, cos\theta\,)^2 = \frac{\epsilon^{\,2}}{4} + \frac{k\lambda}{D}\left(d^2\beta\, cos\theta\,\right)$$

Figure 5 depicts the data points obtained by plotting $d^2\beta\, cos\theta$ values along the x-axis and $(d\beta\, cos\theta\,)^2$ values along the y-axis for TiO_2 nanoparticles. A linear fit to the data points provides the value of D and ε from the slope and y-intercept respectively (Fig. 5). The calculated values have been listed in Table 1.

Halder–Wagner plot

Another very good approach to calculating the structural parameters is the Halder–Wagner (H–W) model given by the following expression[42,43]:

$$\left(\frac{\beta}{tan\theta}\right)^2 = 16\epsilon^{\,2} + \left(\frac{k\lambda}{D}\right)\left(\frac{\beta}{tan\theta\, sin\theta}\right)$$

Figure 5 shows the plot of $\left(\frac{\beta}{tan\theta}\right)^2$ along y-axis against ($\frac{\beta}{tan\theta\, sin\theta}$) along x-axis. A linear fit to the data points yields the values of D and ε from the slope and intercept of the graph respectively and are tabulated in Table 1.

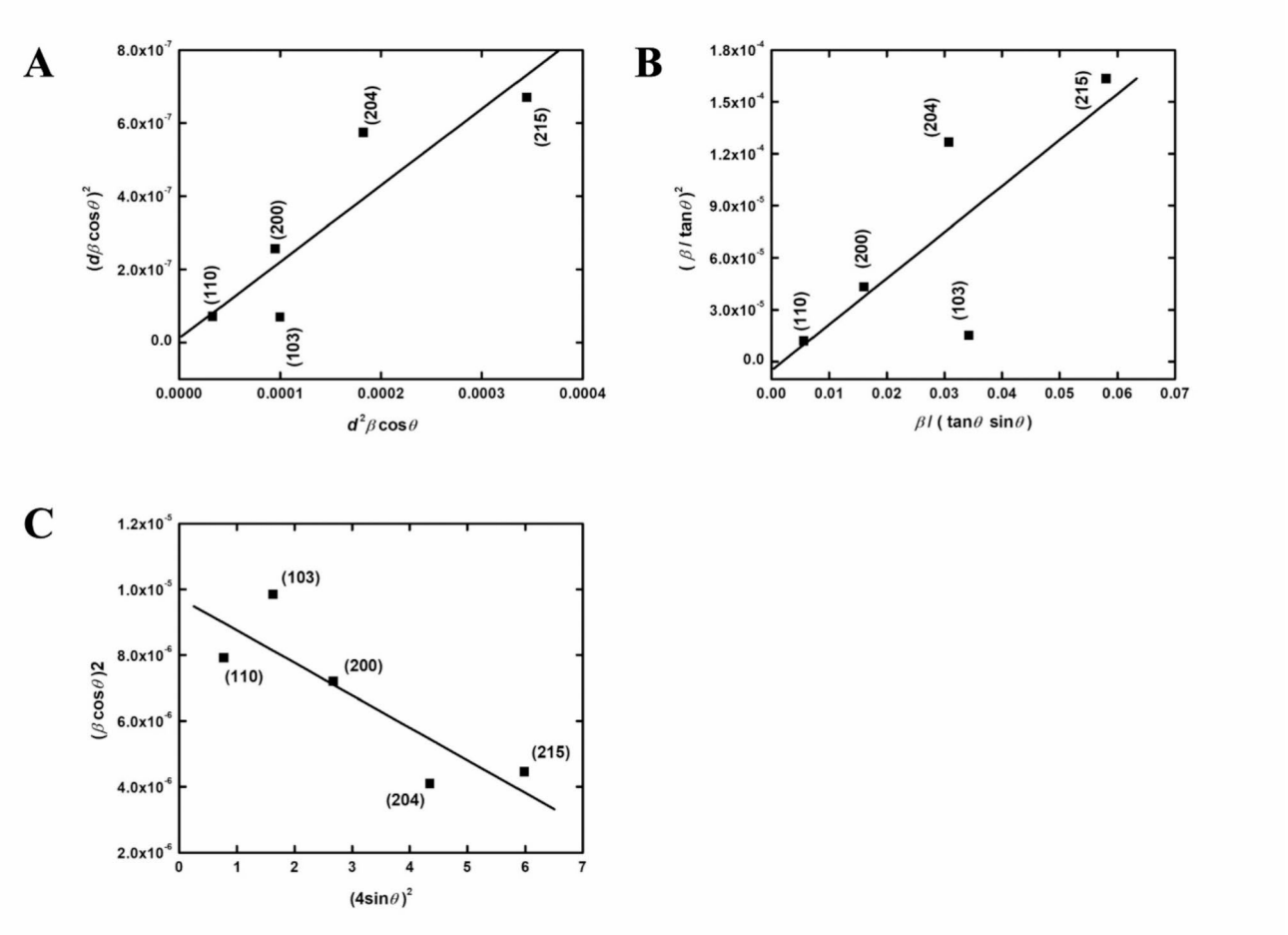

Fig. 5. Size-Strain plot (**a**), Halder-Wagner plot (**b**), and Wagner-Aqua plot (**c**) for TiO_2 nanoparticles.

Wagner–Aqua model

Wagner and Aqua also devised an analytical approach to calculate the structural parameters using the following expression[44,45]:

$$(\beta\cos\theta)^2 = \left(\frac{k\lambda}{D}\right)^2 + (4\epsilon\sin\theta)^2$$

Figure 5 depicts the W–A model utilizing $(\beta\cos\theta)^2$ vis a vis $(4\sin\theta)^2$, in which straight-line fit to the data points will provide *D* and ε from the intercept and slope respectively also illustrated in Table 1.

Insecticidal activity bioassay

Green synthesized TiO_2 NPs showed significant insecticidal activity against DCB when checked at their 2nd instar nymph, 4th instar nymph, and adult stage. The overall percentage of mortality was found directly proportional to the concentration of synthesized nanoparticles used (Tables 2, 3 and 4). At the highest tested concentration of 1500 ppm, after 96 h, percentage mortality remained between 90 and 95% with the highest in 2nd instar nymphs and the lowest in adults. Following this, lower concentrations of 1200 and 900 ppm also produced highly significant results. In 4th instar nymphs, 88% mortality was recorded after 96 h which was 83% higher than the control and 7% lower than the highest tested concentration of 1500 ppm. Percentage mortality was also found time dependent. The significance level of the treatments sharply increased between 24 and 48 h and after that, the rise in mortality was relatively slower. Nanoparticles in lower concentrations took a longer time to show highly significant results. Whereas the same efficacy was achieved earlier with higher doses, as a tested concentration of 600 ppm showed 71% mortality in 2nd instar nymphs after 96 h, but the same nanoparticles when used in 1500 ppm concentration caused an equal percentage of mortality just after 48 h (Table 2). Similarly in adults, 900 ppm concentration resulted in 70% mortality whereas with an increase in concentration to 1500 ppm same mortality rate was achieved just after 48 h of post-treatment application (Table 4).

Concentration (ppm)	Percentage mortality			
	24 h	48 h	72 h	96 h
300	4.72 ± 2.15^{k}	12.75 ± 0.75^{j}	20.72 ± 1.15^{i}	27.26 ± 1.33^{h}
600	11.28 ± 1.25^{j}	29.73 ± 1.82^{h}	54.33 ± 1.44^{f}	71.27 ± 0.52^{d}
900	15.64 ± 0.72^{j}	39.14 ± 2.23^{g}	65.48 ± 0.57^{e}	85.03 ± 1.75^{b}
1200	26.82 ± 1.27^{h}	52.96 ± 0.53^{f}	77.49 ± 2.31^{c}	88.15 ± 2.15^{b}
1500	38.75 ± 1.44^{g}	73.49 ± 1.51^{cd}	88.19 ± 1.28^{b}	95.62 ± 2.94^{a}
Control	0 ± 0.00^{k}	1.06 ± 0.92^{k}	1.78 ± 1.68^{k}	2.52 ± 1.54^{k}

Table 2. Mortality of *Oxycarenus Hyalinipennis* 2nd Instar caused by various concentrations of TiO_2 nanoparticles synthesized by *Calatropis procera* latex at different time intervals. Data is presented as mean ± standard error. Means having the same letter are not significantly different.

Concentration (ppm)	Percentage mortality			
	24 h	48 h	72 h	96 h
300	3.94 ± 2.15^{no}	5.17 ± 0.75^{n}	11.09 ± 1.15^{lm}	16.47 ± 1.33^{k}
600	9.53 ± 1.25^{m}	21.86 ± 1.82^{j}	41.94 ± 1.44^{h}	53.89 ± 0.52^{f}
900	13.71 ± 0.72^{kl}	35.73 ± 2.23^{i}	58.54 ± 0.57^{e}	68.07 ± 1.75^{d}
1200	22.73 ± 1.27^{j}	48.73 ± 0.53^{g}	73.42 ± 2.31^{c}	78.64 ± 2.15^{b}
1500	32.64 ± 1.44^{i}	69.48 ± 1.51^{d}	81.26 ± 1.28^{b}	91.53 ± 2.94^{a}
Control	0 ± 0.00^{o}	0.00 ± 0.92^{o}	1.05 ± 1.68^{o}	1.89 ± 1.54^{o}

Table 3. Mortality of *Oxycarenus Hyalinipennis* 4th instar caused by various concentrations of TiO_2 nanoparticles synthesized by *Calatropis procera* latex at different time intervals. Data is presented as mean ± standard error. Means having the same letter are not significantly different.

Concentration (ppm)	Percentage Mortality			
	24 h	48 h	72 h	96 h
300	4.03 ± 2.15^{k}	5.56 ± 0.75^{k}	9.83 ± 1.15^{j}	12.73 ± 1.33^{i}
600	8.89 ± 1.25^{j}	18.89 ± 1.82^{h}	34.47 ± 1.44^{f}	51.49 ± 0.52^{d}
900	11.64 ± 0.72^{ij}	33.33 ± 2.23^{f}	51.26 ± 0.57^{d}	70.54 ± 1.75^{c}
1200	20.67 ± 1.27^{h}	42.63 ± 0.53^{e}	70.48 ± 2.31^{c}	79.09 ± 2.15^{b}
1500	28.93 ± 1.44^{g}	70.17 ± 1.51^{c}	79.76 ± 1.28^{b}	90.62 ± 2.94^{a}
Control	0 ± 0.00^{l}	0.00 ± 0.00^{l}	0.00 ± 1.68^{l}	0.00 ± 1.54^{l}

Table 4. Mortality of *Oxycarenus Hyalinipennis* adults caused by various concentrations of TiO_2 nanoparticles synthesized by *Calatropis procera* latex at different time intervals. Data is presented as mean ± standard error. Means having the same letter are not significantly different.

Discussion

Green synthesis of metal and metal oxide nanoparticles with bioactive potential has attracted many researchers in recent years and so a reasonable number of studies are available confirming the potential of these nano-sized insecticides against various insect pests. They can also alter the levels of a variety of enzymes and hormones, and delay the developmental processes in insects. This chapter focuses on the synthesis of nanoinsecticides, and their potential application and action mechanism in insects. However, few reports are available against the dusky cotton bug that has emerged as an important cotton pest with several reports of the development of insecticidal resistance in it. This study was therefore designed to investigate the potential of plant-based synthesized TiO_2 NPs against dusky cotton bug as no such earlier reports are available.

The synthesis of TiO_2 NPs was initially confirmed by the color transformation of the solution to a white colloidal solution because of the reduction of Ti ions to TiO_2NPs. This color change was also supported by previous reports[53]. Further confirmation of TiO_2 NPs was done through UV-Vis spectroscopy. The spectra showed a peak at a wavelength of 350 nm, which was found in accordance with previous studies on the synthesis of TiO_2 NPs[54].

These biosynthesized TiO_2 NPs showed significant insecticidal potential against dusky cotton bug. The effect was found directly proportional to the concentration of nanoparticles used and inversely proportional to the age of the insect pest. Javaid, et al.[19] also reported a similar trend when the dusky cotton bug was exposed to silver nanoparticles. They reported that the highest tested concentration of 1250 ppm of silver nanoparticles reduced 4th instar by 91.95%; whereas 5th instar and adults showed a decrease in mortality with a percentage

of 84.40 and 83.15% after 72 h of exposure. TiO_2 NPs synthesized in the present study also showed comparable results to that of silver nanoparticles synthesized by Javaid, et al.[19]. However, the toxicity of nano silver is more documented[55]s whereas, TiO_2 is a well-reported inert material used in many daily life products.

The insecticidal potential of nanoparticles has shown two basic mechanisms of action i.e., direct physical damage and oxidative damage. Earlier reports confirm that TiO_2 NPs can generate reactive oxygen species[56]. Shyam-Sundar, et al.[20] reported that green synthesized TiO_2 NPs can increase the activity of detoxification enzymes and can cause histopathological changes in the midgut of *S. litura*.

Several comparative studies that investigated the potential of different metal NPs including TiO_2 reported higher insecticidal activities when compared to other metal nanoparticles. Chakravarthy, et al.[57] reported a higher potential to control *Spodoptera litura* by Nano-TiO_2 than Cds and Nano-Ag. Similarly, in another study, the entomotoxic efficacy of TiO_2 NPs was found significantly higher than aluminum oxide and zinc oxide NPs when tested against *Sitophilus oryzae*[52]. Hence this can be concluded that TiO_2 NPs can be an effective and safe alternative for the control of crop pests regardless of their species.

Earlier studies also support the positive effect of TiO_2 NPs on plant growth. In a recent investigation Gutiérrez-Ramírez, et al.[28] showed an increase in the growth of tomato with the increase in photosynthetic activity, chlorophyll content, antioxidant enzyme activity, sugar, and amino acid contents in plants treated with TiO_2 NPs. Similarly, Servin, et al.[9] reported that *Cucumis sativus* L. grown in the presence of TiO_2 NPs showed an increase in catalase and chlorophyll content of leaves and a significant increment in potassium and phosphorus. Keeping all these reports in view it can be stated that TiO_2 NPs can be used as a safe source for controlling insect pests in crops like cotton.

Conclusion

The green synthesized TiO_2 NPs under laboratory conditions showed a high insecticidal effect after 96 h, with over 90% mortality at a concentration above 1500 ppm to control 2nd Instar nymph of (*Oxycarenus* Spp.). Whereas in the case of 4th Instar 88% mortality was observed at an exposure of 96 h at the same concentration i.e., 1500 ppm. It can further be concluded that amorphous nano-TiO_2 has been successfully synthesized from *C. procera* Latex and it exhibited encouraging results as a biogenic insecticide. However, more research is needed to study the possible implications of the use of TiO_2 NPs for agricultural applications.

Methodology

Preparation of *Calatropis procera* extract

Latex was collected in a clean tube by breaking the *C. procera* stems, collected from botanical garden of University of the Punjab, Lahore, Pakistan. The obtained latex was diluted with distilled water (1:1, v/v). It was mixed well and then centrifuged at 15,000 × *g* at 4 °C for 10 min. It was separated into three layers: rubber, serum, and lipids.

Preparation of titanium dioxide nanoparticles from *C. procera* serum extract

Aqueous Titanium tetraisopropoxide (0.2 M) was added to 50 mL of 3% *C. procera* serum in (1:1). Then the mixture was stirred by a magnetic stirrer at the rate of 6000 rpm (approx. 4020 *g*) for one hour. Following this, the mixture was centrifuged at 4000 rpm for 20 min. The pellet was collected and washing was done to remove the impurities. pH of the solution was adjusted to 7 using 0.1 N sodium hydroxide and 0.1 N hydrochloride solution. After washing the pellet, the solution was again centrifuged at 4000 rpm (approx. 1780 *g*) for 20 min. The pellet was collected and the upper portion of the solution was discarded. The pellet was mixed with distilled water and placed in a hot air oven at 150 ℃ for 2 h. After complete drying, the pellet was then converted into fine powder (Fig. 6). The fine nanoparticle powder was stored at room temperature in an amber-colored sample vial till further use.

Characterization of NPs

The structural properties of the prepared nanoparticles were studied using an X-ray diffractometer (X'pert PANalytical) (CuKα radiation of wavelength 1.5406 Å) operating at 40 kV and a current of 40 mA. XRD patterns were recorded at a scan speed of 4°/min in the 2θ range 20° — 80°.

Collection and rearing of dusky cotton bug DCB

The dusky cotton bug (DCB) population was collected from the Cotton Research Area, Department of Plant Pathology, Faculty of Agricultural Sciences, University of the Punjab, Lahore, Pakistan during October 2023. The 2nd instar nymphs, 4th instar nymphs and adults[58] used in this research were obtained directly from an organic cotton field where only yellow sticky traps were used for sampling and control resulting rare/minimal chances for cross-contamination between the different stages of insects, the collected insects were kept in glass petri dishes separately in Insecticides and Weedicides Resistance Laboratory, Department of Entomology, Faculty of Agricultural Sciences, University of the Punjab. The bulk population of the dusky cotton bug was reared in plastic jars (12 × 6 inches) which were covered with cloth to ensure air flow. The natural diet of cotton bolls comprising cotton lint and fresh twigs of cotton (*Gossypium hirsutam* Linnaeus) was provided. Fresh twigs were substituted for dried twigs thrice a week to keep the culture fresh. DCB F1 homogeneous population was obtained in the Insecticides and Weedicides Resistance Laboratory at 27 ± 2 °C, 60 ± 5% relative humidity, and a photoperiod of 14:10 (L: D) hours[11].

Experiment layout

The TiO_2 NPs were synthesized in the Department of Plant Pathology, Faculty of Agricultural Sciences, University of the Punjab, Lahore. The bioassay was performed at the Insecticides and Weedicides Resistance Laboratory,

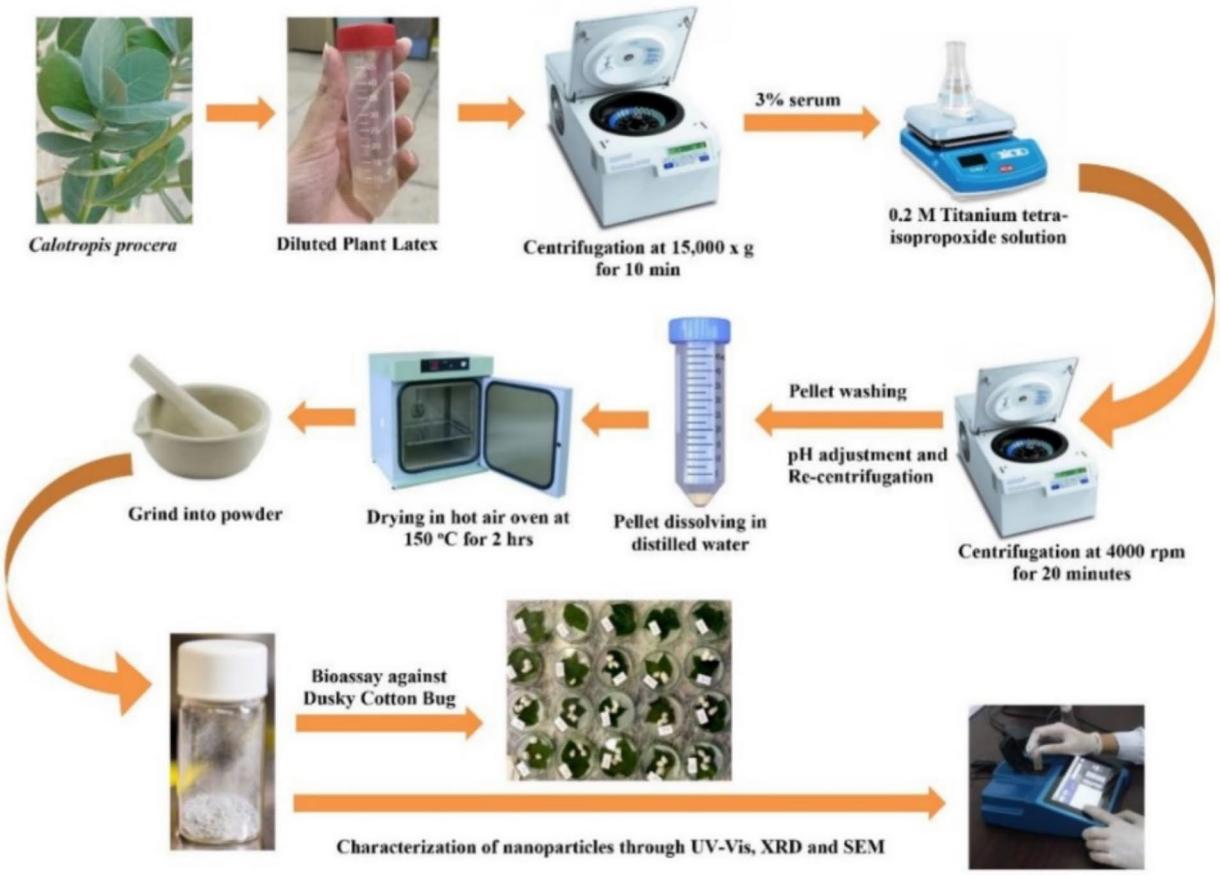

Fig. 6. Scheme for the green synthesis of nanoparticles.

Department of Entomology, Faculty of Agricultural Sciences, University of the Punjab, for the determination of efficacy of TiO_2 against the 2nd and 4th nymphal instars, as well as adult DCB.

Evaluation of insecticidal activity

To investigate the efficacy of TiO_2 NPs, the bioassay was performed by using the leaf dip method as described by Ullah, et al.[11]. The experiment was conducted using Complete Randomized Design (CRD) with three replications. Four concentrations (600, 900, 1200, and 1500 ppm) of TiO_2 NPs were prepared and in control distilled water was used[28]. Leaf discs were prepared and dipped for 10 s in each concentration and were dried at room temperature for 2–3 h, before placing on petri dishes[59]. The size of the petri dish was 5 cm in diameter and these petri dishes were lined with filter paper (Whatman no. 1). To avoid desiccation, filter paper was kept moist under the leaves. Large leaves were utilized to completely cover the petri dishes. Fifteen adult DCB, ten 2nd instar nymphs, and ten 4th instar nymphs were released in each Petri plate, and in each concentration, total of 80 DCB were exposed. There were 300 adults, 200 2nd instar nymphs, and 200 4th instar nymphs in total in this experiment. Cotton leaves were utilized in the control group, which were replicated three times with fifteen DCB, ten 2nd instar nymphs, and ten 4th instars in each Petri plate. The bioassay was carried out under typical lab conditions of 27 ± 2 °C, 60 ± 5% relative humidity, and a photoperiod of 14:10 (L: D) hours. DCB mortality data was collected after 24, 48, 72, and 96 h post-treatment application and considered dead if they did not move with the use of a fine camel hair brush[11].

Data analysis

The data were analyzed statistically performing analysis of variance (ANOVA) and Duncan's New Multiple Range test (DNMRT) at 5% level of significance using Excel software add in DSAASTAT developed by Onofri (Italy).

Data availability

Data is provided within the manuscript file.

Received: 20 July 2024; Accepted: 9 December 2024
Published online: 01 April 2025

References

1. Samy, O. A revision of the African species of Oxycarenus (Hemiptera: Lygaeidae). *Trans. Royal Entomol. Soc. Lond.* **121**, 79–165 (1969).
2. Smith, T. R. & Brambila, J. A major pest of cotton, *Oxycarenus Hyalinipennis* (Heteroptera: Oxycarenidae) in the Bahamas. *Fla. Entomol.* **91**, 479–482 (2008).
3. Baranowski, R. M. & Slater, J. A. *Lygaeidae of the West Indies* (Agricultural Experiment Station, Institute of Food and Agricultural Sciences, 2005).
4. Sanghi, A. H., Aslam, M. & Khalid, L. Efficacy of different insecticides against dusky cotton bug *Oxycarenus Hyalinipennis* (Hemiptera: Lygaeidae) in ecological zone of Rahim Yar Khan. *Int. J. Compr. Res. Biol. Sci.* **1**, 49–54 (2014).
5. Waqar Jaleel, W. J., Saeed, S., Naqqash, S. S., Zaka, S. & M. & Survey of Bt cotton in Punjab Pakistan related to the knowledge, perception and practices of farmers regarding insect pests. *Int. J. Agric. Crop Sci.* **7**, 10–20 (2014).
6. Sammaiah, C., Laxman, P. & Samatha, C. Study on infestation of cotton insect stainers on BT-cotton and non BT-cotton in Warangal, Andhra Pradesh. *Int. J. Environ. Sci.* **3**, 1155–1160 (2012).
7. Khan, M. A. et al. Assessment of density-dependent feeding damage by the cotton dusky bug, *Oxycarenus Laetus* Kirby (Hemiptera: Lygaeidae), in cotton. *Turkish J. Agric. Forestry*. **38**, 198–206 (2014).
8. Sewify, G. & Semeada, A. Effect of population density of the cotton seed bug, *Oxycarinus Hyalinipennis* Costa, on yield and oil content of cotton seeds. *Bull. Fac. Agriculture-Cairo Univ.* **44**, 445–452 (1993).
9. Servin, A. D. et al. Synchrotron verification of TiO_2 accumulation in cucumber fruit: a possible pathway of TiO_2 nanoparticle transfer from soil into the food chain. *Environ. Sci. Technol.* **47**, 11592–11598 (2013).
10. Abbas, G., Hassan, N., Haq, I., Farhan, M. & Karar, H. Relative suitability of various insecticide for early crop management of cotton against sucking insect pest complex especially dusky cotton bug *Oxycarenus Hyalinipennis* (Hemiptera: Oxycarenidae). *Pakistan Entomol.* **36**, 129–133 (2014).
11. Ullah, S., Shad, S. A. & Abbas, N. Resistance of dusky cotton bug, *Oxycarenus Hyalinipennis* Costa (Lygaidae: Hemiptera), to conventional and novel chemistry insecticides. *J. Econ. Entomol.* **109**, 345–351 (2016).
12. Ijaz, M. & Shad, S. A. Realized heritability, cross-resistance and high risk of resistance development to spirotetramat in dusky cotton bug, *Oxycarenus Hyalinipennis* Costa (Hemiptera: Lygaeidae), an emerging threat to BT cotton in Pakistan. *Phytoparasitica* **50**, 453–463 (2022).
13. Elrehawy, E. S. & ElDoksch, H. A. The insecticidal and antifeedant activity of *Calotropis procera* latex and foliar extracts against the red palm weevil, *Rhynchophorus Ferrugineus* (Olivier)(Coleoptera: Curculionidae). *Egypt. Acad. J. Biol. Sci. F Toxicol. Pest Control.* **14**, 25–33 (2022).
14. Kumar, D., Ranjan, A., Chauhan, A., Prakash, D. & Jindal, T. Insecticidal activities of different extracts of *Calotropis procera*. *New. Front. Environ. Toxicol.* 91–102 (2022).
15. Luzala, M. M. et al. A critical review of the antimicrobial and antibiofilm activities of green-synthesized plant-based metallic nanoparticles. *Nanomaterials* **12**, 1841 (2022).
16. Mustapha, T., Misni, N., Ithnin, N. R. & Daskum, A. M. Unyah, N. Z. A review on plants and microorganisms mediated synthesis of silver nanoparticles, role of plants metabolites and applications. *Int. J. Environ. Res. Public Health*. **19**, 674 (2022).
17. Saka, A. et al. Biosynthesis of TiO_2 nanoparticles by Caricaceae (papaya) shell extracts for antifungal application. *Sci. Rep.* **12**, 15960 (2022).
18. Sunny, N. E. et al. Green synthesis of titanium dioxide nanoparticles using plant biomass and their applications-A review. *Chemosphere* **300**, 134612 (2022).
19. Javaid, M. et al. Characterization of *Azadirachta indica* synthesized silver nanoparticles and its toxicity against Dusky cotton bug, *Oxycarenus Hyalinipennis* Costa (Hemiptera: Lygaeidae). *Int. J. Trop. Insect Sci.* **43**, 463–473 (2023).
20. Shyam-Sundar, N. et al. Eco-friendly biosynthesis of TiO_2 nanoparticles using *Desmostachya bipinnata* extract: Larvicidal and pupicidal potential against *Aedes aegypti* and *Spodoptera litura* and acute toxicity in non-target organisms. *Sci. Total Environ.* **858**, 159512 (2023).
21. Hsu, C. Y. et al. Nano titanium oxide (nano-TiO_2): a review of synthesis methods, properties, and applications. *Case Stud. Chem. Environ. Eng.*, **100626** (2024).
22. Suhag, R. et al. Fruit peel bioactives, valorisation into nanoparticles and potential applications: a review. *Crit. Rev. Food Sci. Nutr.* **63**, 6757–6776 (2023).
23. Vieira, I. R. S., de Carvalho, A. P. A. & Conte-Junior, C. A. d. Recent advances in biobased and biodegradable polymer nanocomposites, nanoparticles, and natural antioxidants for antibacterial and antioxidant food packaging applications. *Comprehensive Rev. Food Sci. Food Saf.* **21**, 3673–3716 (2022).
24. Eddy, D. R. et al. A review of recent developments in green synthesis of TiO_2 nanoparticles using plant extract: synthesis, characterization and photocatalytic activity. *Inorg. Chem. Commun.* 112531 (2024).
25. Nor, S. M. & Ding, P. Trends and advances in edible biopolymer coating for tropical fruit: a review. *Food Res. Int.* **134**, 109208 (2020).
26. Verma, V. et al. A review on green synthesis of TiO_2 NPs: photocatalysis and antimicrobial applications. *Polymers* **14**, 1444 (2022).
27. Rajam, R. P., Kannan, S. & Kajendran, D. Cosmeceuticals an emerging technology—A review. *World J. Pharm. Res.* **8**, 664–685 (2019).
28. Gutiérrez-Ramírez, J. A. et al. Insecticidal effect of zinc oxide and titanium dioxide nanoparticles against *Bactericera Cockerelli* Sulc. (Hemiptera: Triozidae) on tomato Solanum lycopersicum. *Agronomy* **11**, 1460 (2021).
29. Hilal, S. M., Mohmed, A. S., Barry, N. M. & Ibrahim, M. H. In *IOP Conference Series: Earth and Environmental Science.* 012088 (IOP Publishing).
30. Sabbour, M. *Pests and Plant Protection Dep* (National Research Centre, 2012).
31. Kumar, A. & Pandey, G. Synthesis of La: Co: TiO_2 nanocomposite and photocatalytic degradation of tartaric acid in water at various parameters. *Am. J. Nano Res. Appl.* **5**, 40–48 (2017).
32. Al-Taweel, S. S. & Saud, H. R. New route for synthesis of pure anatase TiO_2 nanoparticles via utrasound-assisted sol-gel method. *J. Chem. Pharm. Res.* **8**, 620–626 (2016).
33. Kumaraswamy, J. et al. Thermal analysis of Ni-Cu alloy nanocomposites processed by sand mold casting. *Adv. Mater. Sci. Eng.* **2022**, 2530707 (2022).
34. Alonizan, N. et al. Photocatalytic activity, microstructures and luminescent study of Ti-ZS: M nano-composites materials. *J. Inorg. Organomet. Polym Mater.* **30**, 4372–4381 (2020).
35. El-Sherbiny, S., Morsy, F., Samir, M. & Fouad, O. A. Synthesis, characterization and application of TiO_2 nanopowders as special paper coating pigment. *Appl. Nanosci.* **4**, 305–313 (2014).
36. Homann, T., Bredow, T. & Jug, K. Adsorption of small molecules on the anatase (1 0 0) surface. *Surf. Sci.* **555**, 135–144 (2004).
37. Scherrer, P. Abschätzungen Von Charaktersummen, Einheit Und Klassenzahlen. *Göttinger Nachr. Gesell.* **2**, 98 (1918).
38. Heiba, Z. K., Mohamed, M. B. & Badawi, A. Impact of preparation temperature on the structure, optical and electronic characteristics of Zn0. 9V0. 1S nanoparticles with Williamson-Hall model mechanistic view. *Appl. Phys. A.* **128**, 456 (2022).
39. Williamson, G. & Hall, W. X-ray line broadening from filed aluminium and wolfram. *Acta Metall.* **1**, 22–31 (1953).
40. Das, R. & Sarkar, S. X-ray diffraction analysis of synthesized silver nanohexagon for the study of their mechanical properties. *Mater. Chem. Phys.* **167**, 97–102 (2015).

41. Prince, E., Prince, E. & Stalick, J. *Accuracy in Powder Diffraction II* (US Department of Commerce, National Institute of Standards and Technology, 1992).
42. Halder, N. & Wagner, C. Separation of particle size and lattice strain in integral breadth measurements. *Acta Crystallogr. A*. **20**, 312–313 (1966).
43. Sen, S. K. et al. Effect of Fe-doping and post annealing temperature on the structural and optical properties of MoO_3 nanosheets. *J. Mater. Sci.: Mater. Electron.* **30**, 14355–14367 (2019).
44. Paul, T. C. & Podder, J. Synthesis and characterization of Zn-incorporated TiO_2 thin films: impact of crystallite size on X-ray line broadening and bandgap tuning. *Appl. Phys. A*. **125**, 818 (2019).
45. Wagner, C. & Aqua, E. Analysis of the broadening of powder pattern peaks from cold-worked face-centered and body-centered cubic metals. *Adv. X-Ray Anal.* **7**, 46–65 (1963).
46. Aftab, M., Butt, M., Ali, D., Bashir, F. & Aftab, Z. Impact of copper doping in NiO thin films on their structure, morphology, and antibacterial activity against *Escherichia coli*. *Ceram. Int.* **46**, 5037–5049 (2020).
47. Konan, F. K., Hartiti, B., Batan, A. & Aka, B. X-ray diffraction, XPS, and Raman spectroscopy of coated ZnO: Al (1–7 at%) nanoparticles. *E-J. Surf. Sci. Nanotechnol.* **17**, 163–168 (2019).
48. Munawar, T. et al. Rare earth metal co-doped Zn0· 9La0. 05M0. 05O (M = yb, sm, nd) nanocrystals; energy gap tailoring, structural, photocatalytic and antibacterial studies. *Mater. Sci. Semiconduct. Process.* **122**, 105485 (2021).
49. Biju, V., Sugathan, N., Vrinda, V. & Salini, S. Estimation of lattice strain in nanocrystalline silver from X-ray diffraction line broadening. *J. Mater. Sci.* **43**, 1175–1179 (2008).
50. Mote, V. D., Purushotham, Y. & Dole, B. Williamson-Hall analysis in estimation of lattice strain in nanometer-sized ZnO particles. *J. Theoretical Appl. Phys.* **6**, 1–8 (2012).
51. Zak, A. K., Yousefi, R., Majid, A., Muhamad, M. & W. H. & Facile synthesis and X-ray peak broadening studies of Zn1 – xMgxO nanoparticles. *Ceram. Int.* **38**, 2059–2064 (2012).
52. Das, S., Yadav, A. & Debnath, N. Entomotoxic efficacy of aluminium oxide, titanium dioxide and zinc oxide nanoparticles against *Sitophilus oryzae* (L.): a comparative analysis. *J. Stored Prod. Res.* **83**, 92–96 (2019).
53. Helmy, E. A. M., San, P. P., Zhang, Y. Z., Adarkwah, C. & Tuda, M. Entomotoxic efficacy of fungus-synthesized nanoparticles against immature stages of stored bean pests. *Sci. Rep.* **13**, 8508 (2023).
54. Vijayalakshmi, R. & Rajendran, V. Synthesis and characterization of nano-TiO2 via different methods. *Archives Appl. Sci. Res.* **4**, 1183–1190 (2012).
55. Zhang, J. et al. Nano silver-induced toxicity and associated mechanisms. *Int. J. Nanomed.*, 1851–1864 (2022).
56. Tourinho, P. S. et al. Metal-based nanoparticles in soil: Fate, behavior, and effects on soil invertebrates. *Environ. Toxicol. Chem.* **31**, 1679–1692 (2012).
57. Chakravarthy, A. et al. Bio efficacy of inorganic nanoparticles CdS, Nano-Ag and Nano-TiO_2 against *Spodoptera litura* (Fabricius) (Lepidoptera: Noctuidae). *Curr. Biotica*. **6**, 271–281 (2012).
58. Muthyala Srinivas, M. S. & Patil, B. Quantitative and qualitative loss caused by dusky cotton bug, *Oxycarenus laetus* Kirby on cotton. (2004).
59. Pavitra, G., Sushila, N., Sreenivas, A., Ashok, J. & Sharanagouda, H. Biosynthesis of green silica nanoparticles and its effect on cotton aphid, *Aphis gossypii* Glover and mealybug, *Phenacoccus Solenopsis* Tinsley. *Int. J. Curr. Microbiol. Appl. Sci.* **7**, 1450–1460 (2018).

Author contributions

M.F., M.M. and G.N. Performed experiment and wrote the manuscript M.A worked on characterization of Nanoparticles and wrote manuscriptT.A., Z.e.A. and W.A. supervised experiment and wrote the manuscriptH.R data analysis and wrote manuscriptN.A. B. data analysis and funding of the whole project.Z.e.A. is Primary corresponding author of the manuscriptG.L Helped in Data analysis Revision of the manuscript.

Funding

This research was funded by Researchers Supporting Project (RSPD2025R1048), King Saud University, Saudi Arabia.

Declarations

Competing interests

The authors declare no competing interests.

Additional information

Correspondence and requests for materials should be addressed to M.A. or Z.-e.-H.A.

Reprints and permissions information is available at www.nature.com/reprints.

Publisher's note Springer Nature remains neutral with regard to jurisdictional claims in published maps and institutional affiliations.